series of tests was 18,000 Btu/lbm. This is not a MAARC limit but a system limit.

As the mass flow increases, the voltage and fraction of power lost to the cathode is constant or increases slightly. The anode loss decreases with increasing mass flow, thus the over-all efficiency of the device increases.

Figure 3 shows the variation of the over-all efficiency of the device with total power and includes data from other facilities. These earlier data indicate that the efficiency increases with power achieving an efficiency above 95% at the 100 Mw level. This trend is verified in the present device using both copper and tungsten cathodes. An efficiency of 70% is obtained at 0.4 Mw using the copper cathode, and 85% is obtained at 0.2 Mw using the tungsten cathode.

Three sets of consecutive frames taken from the high-speed films of the discharge are shown in Fig. 4. Each set is typical of the discharge at the operating conditions specified. Set "a" was taken at a field strength of $B = 0.265$ tesla, current $I = 760$ amp, and a mass flow of $\dot{m} = 0.014$ lbm/sec. At this condition, the discharge consists of a concentrated current path, or "spoke," and is typical of the discharge in conventional arc heaters. The spoke rotated at a measured frequency of 3180 Hz. Assuming that the spoke rotates with the bulk gas, an expression for the rotational frequency can be derived as $\omega = IB/\dot{m}2\pi(r_o^2 - r_i^2)/(r_o^2 + r_i^2)$ where r_i and r_o are the inner and outer electrode radii, respectively. This yields a frequency of 1509 Hz for this device. If the discharge occurs at the cathode tip, then $r_i \sim 0$ and one obtains a frequency of 5060 Hz. These values bracket the measured frequency indicating that the discharge originates somewhere between the tip and the outer surface of the cathode.

In order for the discharge to completely fill the annulus between cathode and anode, i.e., become diffuse, the time for the spoke to make one rotation ($\tau_{rot} = 1/\omega$) must be much less than the residence time (τ_{res}) and/or the characteristic time for recombination (τ_{rec}). For the conditions of this experiment $\tau_{rec} \approx 1{,}000$ μsec, $\tau_{res} \approx 200$ μsec, and for condition "a" $\tau_{rot} \approx 400$ μsec. The criteria for a diffuse discharge are not met.

The visible current path appears to fluctuate between a spoke and a diffuse discharge for the conditions of set b. Although the time to make one revolution is 70 μsec, the current is apparently not high enough to sustain a steady diffuse discharge.

The calculated rotational time for set c is 30 μsec, which is less than the recombination and the residence time, and the necessary conditions for a diffuse discharge are present.

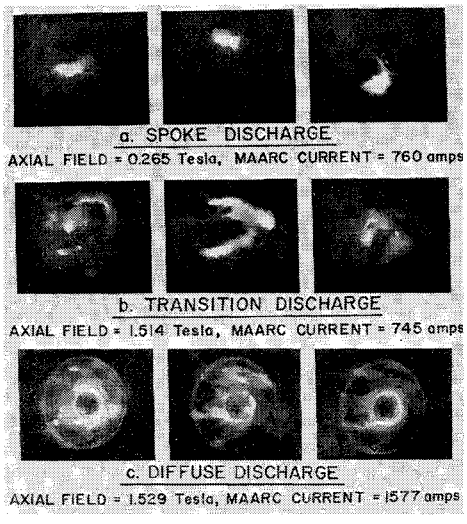

Fig. 4 Consecutive high-speed photographs of the MAARC discharge between the center cathode and coaxial anode (frame rate ≈10,000 frames/sec, shutter speed ≈2 μsec, copper electrodes).

Also, the camera will stop a spoke rotating at 500,000 Hz ($\tau_{rot} \approx 2$ μsec) but no confirmed current path is detected. Hence, the discharge shown in set c is considered diffuse.

Although the magnetic fields utilized were relatively low, the performance obtained with the MAARC indicated that successful operation at atmospheric pressure is possible. The basic criteria are fulfilled for the operation of a MAARC providing supersonic flow with high stagnation pressure and high enthalpy. A MAARC of improved design is being fabricated with the goal of operation at these conditions.

References

[1] Patrick, R. M. and Schneiderman, A. M., "Performance Characteristics of a Magnetic Annular Arc," *AIAA Journal*, Vol. 11, No. 2, Feb. 1966, pp. 283–290.

[2] Patrick, R. M. and Pugh, E. R., "Laboratory Simulation of Solar Wind Phenomena," *Proceedings of Sixth Gas Dynamics Symposium*, Aug. 1965; also AIAA Paper 65-625, 1965, Evanston, Ill.

[3] Schneiderman, A. M., Pugh, E. R., and Patrick, R. M. "Magnetic Annular Arc-Driven Shock Tube," *The Physics of Fluids*, Vol. 11, No. 2, Feb. 1968, pp. 278–294.

[4] Buhler, R. D., Lenn, P., and Richter, R., "Axisymmetric Hall-Arc Jet Wind Tunnel Driver Study," TR 66-213, April 1967, Air Force Flight Dynamics Lab., Wright-Patterson Air Force Base, Ohio.

Bending Stress at a Clamped Support of an Impulsively Loaded Conical Shell

D. B. Longcope* and M. J. Forrestal†
Sandia Laboratories, Albuquerque, N. Mex.

In this Note, a perturbation solution is developed for the bending stress at a clamped support of a semi-infinite, conical shell subjected to a uniform, normal impulse. The response is described by the shell-bending theory which neglects transverse-shear deformation and rotary inertia. In Ref. 1, this theory was shown to adequately predict the maximum bending stress at a clamped support of an impulsively loaded, circular, cylindrical shell.

The small perturbation parameter is $\sin\alpha$ where α is the half apical angle shown in Fig. 1. It is shown that the bending stress history for a conical shell with a small half apical angle closely follows the bending stress history for a circular, cylindrical shell.

Shell Equations of Motion

Equations for the axisymmetric motion of a conical shell are recorded in Ref. 2. With the slant coordinate x defined

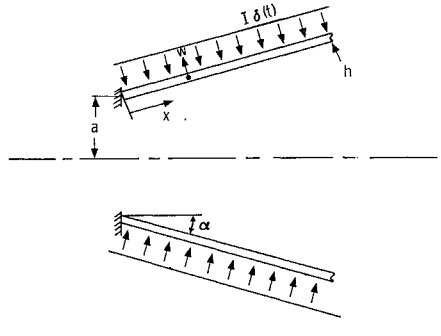

Fig. 1 Geometry of the problem.

Received April 30, 1970; revision received May 25, 1970. This work was supported by the U.S. Atomic Energy Commission.

* Staff Member.
† Staff Member. Member AIAA.

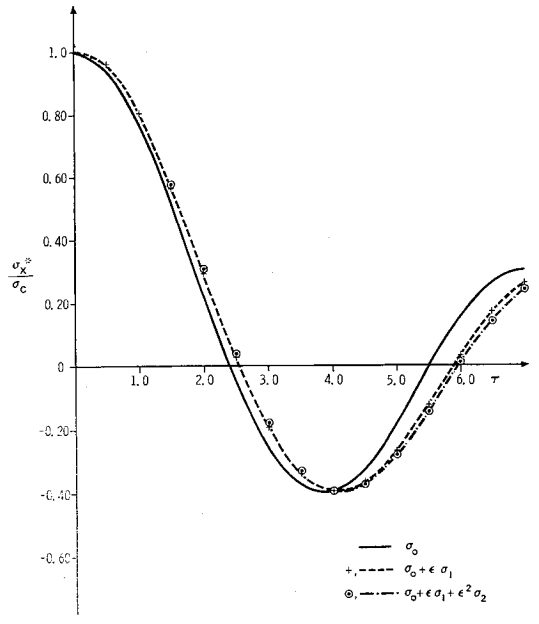

Fig. 2 Bending stress at the radially outward shell surface for $\eta = 0$, $\alpha = 10°$, $a/h = 10$.

in Fig. 1 and the slant displacement component taken as zero, the equations presented in Ref. 2 reduce to

$$(1 + \eta\sin\alpha)^3\frac{\partial^4 W}{\partial\eta^4} + 2\sin\alpha(1 + \eta\sin\alpha)^2\frac{\partial^3 W}{\partial\eta^3} - \sin^2\alpha(1 + \eta\sin\alpha)\frac{\partial^2 W}{\partial\eta^2} + \sin^3\alpha\frac{\partial W}{\partial\eta} + \frac{\cos^2\alpha}{b^2}(1 + \eta\sin\alpha)W = -\frac{(1 + \eta\sin\alpha)^3}{b^2}\times\left[\frac{\partial^2 W}{\partial\tau^2} + \frac{(1 - \nu^2)cI}{Eh}\delta(\tau)\right] \quad (1a)$$

$$W = w/a,\ \eta = x/a,\ \tau = ct/a,\ c^2 = E/\rho(1 - \nu^2),\ b^2 = h^2/12a^2 \quad (1b)$$

where a is the shell radius at the clamped support and h is the shell thickness; E, ν, and ρ are Young's modulus, Poisson's ratio, and density; w is the normal displacement component, measured positive outward; t is time; I is the impulse intensity; and $\delta(\tau)$ is the Dirac delta function.

The bending moment M_x and magnitude of bending stress $\sigma_x{}^*$ at the surfaces of the shell are related to W by

$$M_x = \frac{-Eh^3}{12(1 - \nu^2)a}\left(\frac{\partial^2 W}{\partial\eta^2} + \frac{\nu\sin\alpha}{1 + \eta\sin\alpha}\cdot\frac{\partial W}{\partial\eta}\right) \quad (2a)$$

$$\sigma_x{}^* = \pm 6M_x/h^2 \quad (2b)$$

where the plus and minus signs refer to the radially outward and inward shell surfaces, respectively.

Perturbation Procedure

The small perturbation parameter is defined as

$$\epsilon = \sin\alpha \quad (3a)$$

and a regular perturbation solution for W is taken in the form

$$W(\eta,\tau) = W_0(\eta,\tau) + \epsilon W_1(\eta,\tau) + \epsilon^2 W_2(\eta,\tau) + \ldots \quad (3b)$$

Substituting Eqs. (3) into Eq. (1a) and setting the coefficients of the different orders of ϵ equal to zero results in the following sequence of equations

$$b^2(\partial^4 W_0/\partial\eta^4) + W_0 + \partial^2 W_0/\partial\tau^2 = -[(1 - \nu^2)cI/Eh]\delta(\tau) \quad (4a)$$

$$b^2(\partial^4 W_1/\partial\eta^4) + W_1 + \partial^2 W_1/\partial\tau^2 = -2b^2(\partial^3 W_0/\partial\eta^3) + 2\eta W_0 \quad (4b)$$

$$b^2\frac{\partial^4 W_2}{\partial\eta^4} + W_2 + \frac{\partial^2 W_2}{\partial\tau^2} = (1 - 3\eta^2)W_0 + b^2\frac{\partial^2 W_0}{\partial\eta^2} + 2\eta b^2\frac{\partial^3 W_0}{\partial\eta^3} - 2b^2\frac{\partial^3 W_1}{\partial\eta^3} + 2\eta W_1 \quad (4c)$$

Substitution of Eq. (3b) into the clamped boundary condition results in the following sequence of boundary conditions

$$W_0 = \partial W_0/\partial\eta = 0 \text{ at } \eta = 0 \quad (5a)$$

$$W_1 = \partial W_1/\partial\eta = 0 \text{ at } \eta = 0 \quad (5b)$$

$$W_2 = \partial W_2/\partial\eta = 0 \text{ at } \eta = 0 \quad (5c)$$

Equations (4) and (5) together with the requirement that W_0, W_1, and W_2 remain bounded as $\eta \to \infty$ form the sequence of boundary-value problems to be solved.

Similarly, the perturbation form of solution for the magnitude of bending stress at the clamped support is

$$\sigma_x{}^* = \pm\frac{Eh}{2(1 - \nu^2)a}\left[\frac{\partial^2 W_0}{\partial\eta^2} + \epsilon\frac{\partial^2 W_1}{\partial\eta^2} + \epsilon^2\frac{\partial^2 W_2}{\partial\eta^2} + \ldots\right] \text{ at } \eta = 0 \quad (6)$$

Response Formula

Equations (4) are reduced to ordinary differential equations by taking a Laplace transform over τ. The solution of these equations subject to quiescent initial conditions are substituted into Eq. (6) to give

$$\bar\sigma_x{}^*/\sigma_c = \pm(\bar\sigma_0 + \epsilon\bar\sigma_1 + \epsilon^2\bar\sigma_2 + \ldots) \text{ at } \eta = 0 \quad (7a)$$

$$\bar\sigma_0 = 1/(1 + s^2)^{1/2} \quad (7b)$$

$$\bar\sigma_1 = \frac{1}{2(3)^{1/4}}\left(\frac{h}{a}\right)^{1/2}\left[\frac{1}{(1 + s^2)^{3/4}} + \frac{5}{2}\frac{1}{(1 + s^2)^{7/4}}\right] \quad (7c)$$

$$\bar\sigma_2 = \frac{h}{8(3)^{1/2}a}\times\left[-\frac{1}{(1 + s^2)} + \frac{39}{(1 + s^2)^2} - \frac{117}{4(1 + s^2)^3} - \frac{48s^2}{(1 + s^2)^3}\right] + \frac{1}{2(1 + s^2)^{3/2}} \quad (7d)$$

where

$$\sigma_c = (3)^{1/2}cI/h \quad (7e)$$

and $\bar\sigma(s)$ is the transform of $\sigma(\tau)$.

Equations (7) are inverted by standard techniques and the shell surface bending stresses at the clamped support are

$$\sigma_x{}^*/\sigma_c = \pm(\sigma_0 + \epsilon\sigma_1 + \epsilon^2\sigma_2 + \ldots) \text{ at } \eta = 0 \quad (8a)$$

$$\sigma_0 = J_0(\tau) \quad (8b)$$

$$\sigma_1 = [(\pi)^{1/2}/2(6)^{1/4}\Gamma(\tfrac{3}{4})](h/a)^{1/2}[\tau^{1/4}J_{1/4}(\tau) + 5/3\tau^{5/4}J_{5/4}(\tau)] \quad (8c)$$

$$\sigma_2 = [1/256(3)^{1/2}]h/a[49\sin\tau - 81\tau\cos\tau - 75\tau^2\sin\tau] + (\tau/2)J_1(\tau) \quad (8d)$$

where $J_n(\tau)$ is a Bessel function of the first kind of order n and $\Gamma(\frac{3}{4})$ is the gamma function with an argument of $\frac{3}{4}$.

Equation (8b) is the response formula for a circular, cylindrical shell which was obtained in Ref. 1.

Discussion and Numerical Result

Formulas for the bending stress at a clamped support of a semi-infinite, conical shell subjected to a uniform, normal impulse have been derived and are given by Eqs. (8). These formulas were developed from a regular perturbation solu-

tion; the small perturbation parameter was $\epsilon = \sin\alpha$, where α is the half apical angle. The solution to the zero equation is that for a circular, cylindrical shell which was presented in Ref. 1. Solutions for the correction terms $\epsilon\sigma_1$ and $\epsilon^2\sigma_2$ are not uniformly valid for large τ because these solutions increase with increasing τ. However, these formulas are a good approximation when the quantity $\epsilon\tau$ is sufficiently small; e.g., see Ref. 3.

The bending stress at the radially outward shell surface at the clamped support for $\alpha = 10°$ and $a/h = 10$ is presented in Fig. 2. The conical response data indicate that one correction term is adequate to describe the conical shell response when $\tau < 4$, during which one relative maximum and one relative minimum are reached. It is only when $\tau > 4$ that the second correction term makes any noticeable difference in the response. These data also indicate that the bending stress history for the conical shell closely follows the bending stress history for the circular, cylindrical shell.

References

[1] Sagartz, M. J. and Forrestal, M. J., "Transient Stresses at a Clamped Support of a Circular Cylindrical Shell," *Journal of Applied Mechanics*, Vol. 36, No. 2, June 1969, pp. 367–369.

[2] Goldberg, J. E., "Axisymmetric Oscillations of Conical Shells," *Proceedings of the Ninth International Congress of Applied Mechanics*, Brussels, Belgium, Vol. 7, Sept. 1956, pp. 333–343.

[3] Cole, J. D., *Perturbation Methods in Applied Mathematics*, Blaisdell, Waltham, Mass., 1968.

Determination of Plasma Drift Velocity by an Ion Acoustic Wave Technique

WILHELM K. REHMANN* AND NOBIE H. STONE†
NASA Marshall Space Flight Center, Huntsville, Ala.

THIS article outlines a method that uses the transmission of ion acoustic waves to determine the drift velocity of a streaming, collisionless N_2^+-plasma, which approximates the ionospheric conditions of ion mass and plasma density.

In a drifting, collisionless plasma, the total ion acoustic wave velocity is the sum of the wave propagation velocity and the plasma drift velocity; i.e., $v_w = v_p + v_d$. Therefore, if v_p is known, the plasma drift velocity can be obtained directly from acoustic wave time-of-flight measurements.

The propagation velocity of longitudinal, ion acoustic waves, as described by Spitzer,[1] is related to other plasma parameters by the equation

$$v_p^2 = (Z\gamma_e kT_e + \gamma_i kT_i)/m_i \quad (1)$$

where Z is the ionic charge, γ_e and γ_i are specific heat ratios, k is Boltzmann's constant, T_e and T_i are electron and ion temperatures, and m_i is the ion mass. Since ion acoustic waves undergo severe Landau damping unless $T_e \gg T_i$, Eq. (1) simplifies to

$$v_p^2 = Z\gamma_e kT_e/m_i \quad (2)$$

which applies to most physical cases of interest.

The method of finding v_d will depend on the ratio, $v_d:v_p$, which, from Eq. (2), is seen to be partially determined by the electron temperature.[2] For the condition that $v_p \approx v_d$, the propagation velocity can be compensated for by measuring

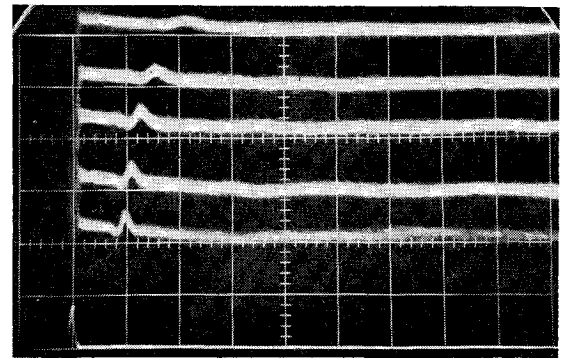

Fig. 1 Upper traces: receiver signals for drift velocities of 11.4 km/sec, 15.2 km/sec, 18.2 km/sec, 20.8 km/sec, and 23.2 km/sec. Transmitting distance, 38 cm: oscilloscope sweep, 17 μsec/cm. Lower trace: driving pulse to emitter.

lapse times of waves traveling over known distances, parallel and perpendicular to the plasma stream.‡ In the event that $v_p \ll v_d$, only a direct measurement of v_w would be required.

To verify this concept, a streaming, collisionless, N_2^+ plasma was generated in a 4 × 8 ft, ultra-high vacuum chamber by a modified, 15 cm Kaufman ion thruster. Neutralization of the N_2^+ ions, produced and accelerated down the axis of the chamber by the thruster, was accomplished by an emissive tantalum wire. The Kaufman thruster was found to be ideal for this purpose in that it afforded a wide range of control over the plasma stream parameters. The plasma density, determined by a shielded Faraday cup, was varied between 10^5 and 10^6 ions/cm^3. The plasma drift velocity, which was calibrated with a 127° electrostatic energy analyzer,[3] was varied from 11.1 km/sec to 23.0 km/sec.

The ion acoustic waves were generated by driving a vertical, 0.03-in. stainless steel wire emitter with a 2-μsec, 50-v pulse at a repetition rate of 60 Hz. The waves were detected downstream by a receiving probe which consisted of a 1.5-in. square stainless steel mesh grid. The use of the wire emitter probe upstream was intended to minimize plasma wake effects in the experiment. The distance between the emitter and receiver probes, which were unbiased, was varied from 11 cm to 47 cm.

Examples of the data obtained are shown in Figs. 1 and 2. The bottom trace in both figures represents the driving pulse to the emitter. The upper traces of Fig. 1 display acoustic waves obtained at a fixed transmitting distance of 38 cm and five different drift velocities. The upper curves of Fig. 2 represent the opposite case where the drift velocity was held constant at 18.2 km/sec and acoustic waves obtained at three different transmitting distances.

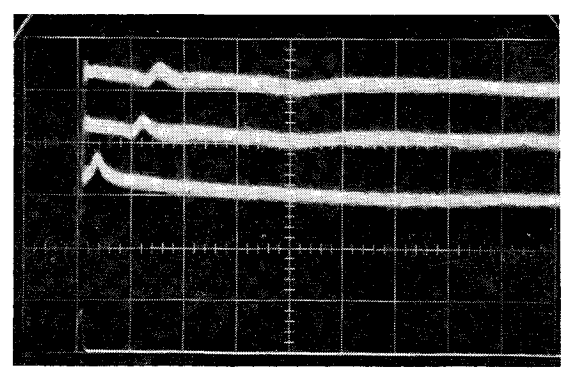

Fig. 2 Upper traces: receiver signals for transmitting distances of 47 cm, 38 cm, and 10.9 cm. Drift velocity: 18.2 km/sec; oscilloscope sweep, 17 μsec/cm. Lower trace: driving signal to emitter.

Received May 13, 1970. The authors would like to express their appreciation to E. Stuhlinger for his supporting interest, and to the National Research Council, which contributed financial support to this work.

* NRC-NAS Resident Research Associate.

† Physicist, Space Sciences Laboratory.

‡ Suggested by L. H. Wood, formerly of Space Sciences Laboratory, Marshall Space Flight Center.